Inorg. Chem. **2007**, *46*, 8460–8462

In Situ Generation of Oxo–sulfidobis(dithiolene)tungsten(VI) Complexes: Active-Site Models for the Aldehyde Ferredoxin Oxidoreductase Family of Tungsten Enzymes

Hideki Sugimoto,* Hiroyuki Tano, Reiko Tajima, Hiroyuki Miyake, Hiroshi Tsukube, Hiromi Ohi, and Shinobu Itoh

Department of Chemistry, Graduate School of Science, Osaka City University, Sumiyoshi-ku, Osaka 558-8585, Japan

Received June 28, 2007

Oxo–sulfidobis(dithiolene)tungsten(VI) complexes were prepared in situ by the reaction of oxobis(dithiolene)tungsten(V) precursors with hydrosulfide (SH^-). The complexes, characterized by UV–vis, electrospray ionization mass spectrometry, IR, and resonance Raman spectroscopies, model the proposed coordination environment and observed hydrolytic reactions of members of the aldehyde ferredoxin oxidoreductase family of tungsten enzymes.

Tungsten has been recognized as an essential element for the enzymatic activity of certain enzymes from hyperthermophilic archaea, which thrive near 100 °C.[1] Tungsten enzymes have been classified into two major families, the formate dehydrogenase (FDH) family and the aldehyde ferredoxin oxidoreductase (AOR) family.[1] The tungsten center of the FDH family has been well characterized by X-ray crystallography and extended X-ray absorption fine structure (EXAFS) analyses[2] as well as by excellent synthetic modeling studies.[3] On the other hand, the precise tungsten environment in the AOR family is still unclear partly because of the high electron density of the tungsten atom and the heterogeneous nature of the molecules in the crystal examined.[4] However, the X-ray crystallographic analysis has revealed that the tungsten(VI) center is coordinated by two pyranopterin dithiolenes and by no protein side chain although additional ligands were not well resolved.[4] On the other hand, the EXAFS result showed the existence of two atoms at 1.7 and 2.0 Å from the tungsten(VI) center,[1,5,6] and the enzymatic activity was found to be enhanced by the addition of sulfide.[5] To account for the above observations, it has been proposed that the tungsten(VI) center of the active site is coordinated by one terminal oxo, one terminal sulfido, and two dithiolenes adopting a six-coordinate structure, as shown in Figure 1.[5] In synthetic modeling studies, a limited number of mononuclear oxo−sulfidotungsten(VI) compounds such as $Cp^*W^{VI}(O)(S)L$ ($L = CH_3^-$ and CH_2SiMe_3),[7,8] $Tp^*W^{VI}(O)(S)L'$ [$L' = Cl^-$, OPh^-, SPh^-, $SePh^-$, $S_2PPh_2^-$, and (−)-mentholate],[9] $W^{VI}(O)(S)(OSiPh_3)_2(Me_4phen)$,[10] $(Ph_4P)[Cp^*W^{VI}(O)(S)(Se)]$,[11] and $(Et_4N)[W^{VI}(O)(S)(OSiPr^i_3)(bdt)]$[12] have been reported. However, these model compounds do not precisely replicate the six-coordinate oxo−sulfidobis(dithiolene)tungsten(VI) structure proposed for the active sites of the tungsten AOR enzymes (Figure 1). Therefore, the individual roles of the oxo, sulfido, and two dithiolenes as well as of the six-coordinate tungsten(VI) structure proposed for the active sites are a subject to be addressed by using more suitable synthetic coumpounds.

Recently, we reported that the five-coordinate molybdenum(IV) complex, $(Et_4N)_2[Mo^{IV}O(bdt)_2]$, is oxidized to the six-coordinate molybdenum(VI) complex, $(Et_4N)_2[Mo^{VI}O_2(bdt)_2]$, in the presence of 2 equiv of OH^- in CH_3CN, where the possible intermediate $(Et_4N)_2[Mo^{V}O(OH)(bdt)_2]$ is successively deprotonated and oxidized.[13] This result stimulated us to investigate the reaction of oxobis(dithiolene)tungsten(V) compounds with SH^- to obtain novel $(Et_4N)_2[W^{VI}(O)(S)(bdt)_2]$ (**1**) and $(Et_4N)_2[W^{VI}(O)(S)(S_2C_2Ph_2)_2]$ (**4**), which are the first oxo−sulfidobis(dithiolene)tungsten(VI) compounds. bdt and $S_2C_2Ph_2$ are two of the dithiolene ligands

* To whom correspondence should be addressed. E-mail: sugimoto@sci.osaka−cu.ac.jp.

(1) Johnson, M. K.; Rees, D. C.; Adams, M. W. W. *Chem. Rev.* **1996**, *96*, 2817.
(2) George, G. N.; Costa, C.; Mourtra, J. J. *J. Am. Chem. Soc.* **1999**, *121*, 2625.
(3) (a) Sung, K-M.; Holm, R. H. *Inorg. Chem.* **2001**, *40*, 4518. (b) Jiang, J.; Holm, R. H. *Inorg. Chem.* **2004**, *43*, 1302. (c) Groysman, S.; Holm, R. H. *Inorg. Chem.* **2007**, *46*, 4090.
(4) (a) Chan, M. K.; Munkund, S.; Kletzin, A.; Adams, M. W. W.; Rees, D. C. *Science* **1995**, *267*, 1463. (b) Hu, Y.; Faham, S.; Roy, R.; Adams, M. W. W.; Rees, D. C. *J. Mol. Biol.* **1999**, *286*, 899.
(5) Johnson, M. K. *Prog. Inorg. Chem.* **2004**, *52*, 213.
(6) Burgmayer, S. J. N. *Prog. Inorg. Chem.* **2004**, *52*, 491.
(7) Ligand abbreviations: Cp* = pentamethylcyclopentadienyl; Tp* = hydrotris(3,5-dimethylpyrazol-1-yl)borate; Me_4phen = 3,4,7,8-tetramethyl-1,10-phenanthroline; bdt = 1,2-benzenedithiolate; $S_2C_2Ph_2$ = 1,2-diphenylethylene-1,2-dithiolate.
(8) Faller, J. W.; Ma, Y. *Organometallics* **1989**, *8*, 609.
(9) (a) Eagle, A. A.; Harben, S. H.; Tiekink, E. R. T.; Young, C. G. *J. Am. Chem. Soc.* **1994**, *116*, 9749. (b) Eagle, A. A.; Tiekink, E. R. T.; George, G. N.; Young, C. G. *Inorg. Chem.* **2001**, *40*, 4563.
(10) Miao, M.; Willer, M. W.; Holm, R. H. *Inorg. Chem.* **2000**, *39*, 2843.
(11) Kawaguchi, H.; Tatsumi, K. *Angew. Chem., Int. Ed.* **2001**, *40*, 1266.
(12) Wang, J.-J.; Groysman, S.; Lee, S. C.; Holm, R. H. *J. Am. Chem. Soc.* **2007**, *129*, 7512.
(13) Sugimoto, H.; Tarumizu, M.; Miyake, H.; Tsukube, H. *Eur. J. Inorg. Chem.* **2006**, 4494.

10.1021/ic7012733 CCC: $37.00 © 2007 American Chemical Society
Published on Web 09/14/2007

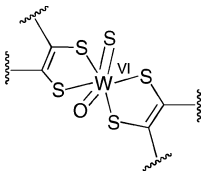

Figure 1. Proposed structure of the active sites of the AOR family.

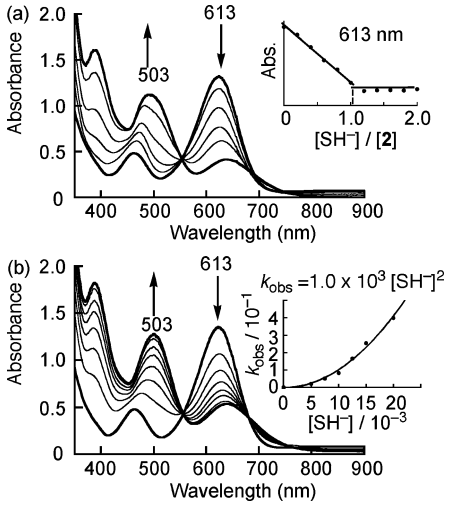

Figure 2. (a) Titration of **2** (4.8×10^{-4} M) with Et_4NSH in C_2H_5CN at −80 °C (inset: plot of the absorption at 613 nm against $[SH^-]/[\mathbf{2}]$). (b) Time-dependent spectral changes for the reaction of **2** (5.0×10^{-4} M) and Et_4NSH (5.0×10^{-3} M) at −80 °C. These spectra were recorded every 12 s (inset: plot of k_{obs} (s^{-1}) vs $[Et_4NSH]$).

employed most often in modeling the active-site structures of tungsten enzymes as well as molybdenum ones.[14] The spectroscopic features and reactivities of the complexes are reported in this Communication.

Figure 2a shows UV−vis spectral changes for the titration of $(Et_4N)[W^VO(bdt)_2]$ (**2**) by Et_4NSH in C_2H_5CN at −80 °C. The intensity of an absorption band centered at 613 nm of **2** decreased with an increase in the new broad absorption bands (392, 503, and 644 nm) in the visible region. The spectral changes were completed when 1 equiv of Et_4NSH was added to the C_2H_5CN solution of **2**. These new bands were different from those of $[W^{VI}O_2(bdt)_2]^{2-}$,[15] $[W^{IV}O(bdt)_2]^{2-}$,[15] $[W(bdt)_3]^{n-}$ (n = 0, 1, and 2),[15b] $[W^{VI}O(S_2)(bdt)_2]^{2-}$,[16] and $[W^{VI}O_2(S)(bdt)]^{2-}$.[12] Figure 2b shows time-dependent spectral changes for the reaction of **2** with 10 equiv of Et_4NSH in C_2H_5CN at −80 °C, where decay of the absorption band at 613 nm of **2** obeyed first-order kinetics (Figure S1 in the Supporting Information; k_{obs} (s^{-1}) = $-\ln\{(A_t - A_\infty)/(A_0 - A_\infty)\}/t$). Interestingly, the apparent first-order rate constant k_{obs} exhibited second-order dependence on the concentration of Et_4NSH, as is clearly shown in the inset of Figure 2b, and the third-order rate constant k for $v = -k[Et_4NSH]^2$ was calculated to be 1.0×10^3 M^{-2} s^{-1}. A CH_3CN solution containing **2** and 1 equiv of SH^- exhibited an electrospray ionization mass spectrometry (ESI-MS) spectrum having peak clusters attributable to $[W^{VI}(O)(S)(bdt)_2]^{2-}$ (**1**) and $[W^{IV}O(bdt)_2]^{2-}$ (**3**) at m/z = 512 and 480 (Figure 3), respectively,[17] and gave no electron paramagnetic resonance (EPR) signal in contrast to the paramagnetic character of **2**. The ^1H NMR spectrum at room temperature of a CD_3CN solution containing **2** and 1 equiv of SH^- also showed sharp

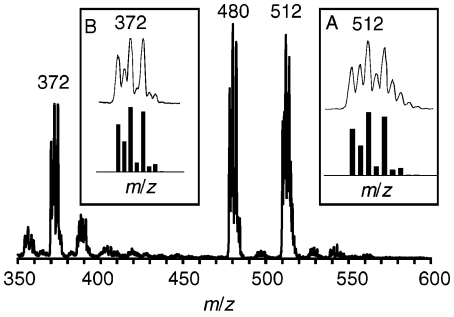

Figure 3. Negative-ion ESI-MS spectrum of a reaction solution of **2** (5.0×10^{-3} M) and 1 equiv of Et_4NSH [insets A and B: observed (above) and calculated (below) isotopic distributions for $[\mathbf{1}-e]^-$ and $[\mathbf{1}-bdt-e]^-$, respectively].

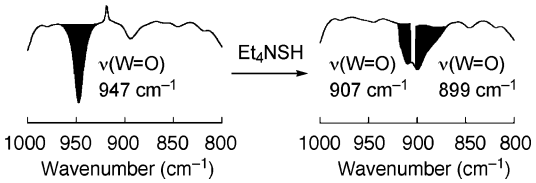

Figure 4. IR spectra of **2** (2.5×10^{-3} M) in CH_3CN (left) and a reaction solution of **2** and 1 equiv of Et_4NSH (right).

signals attributable to an equimolar mixture of **1** and **3** in the diamagnetic region with the expected integration ratios as indicated in ref 18.[18] Furthermore, in the IR spectrum, the strong $\nu(W^V{=}O)$ stretching band at 947 cm^{-1} of **2** disappeared upon treatment with 1 equiv of Et_4NSH and instead two new strong bands appeared at 907 and 899 cm^{-1} (Figure 4). The band at 907 cm^{-1} was identical with a $\nu(W^{IV}{=}O)$ stretching band of an authentic sample of **3** prepared separately. On the basis of the results of UV−vis, ESI-MS, EPR, ^1H NMR, and IR studies, we conclude that **2** is converted into 0.5 equiv of **1** and 0.5 equiv of **3** upon reaction with 1 equiv of SH^-. In such a case, the IR band at 899 cm^{-1} can be assigned to a $\nu(W^{VI}{=}O)$ stretching band of **1**. Another $[W^{VI}(O)(S)]^{2+}$ compound, **4**, was similarly prepared in situ from $(Et_4N)[W^VO(S_2C_2Ph_2)_2]$ (**5**)[21] and Et_4NSH (see Figures S2−S5 in the Supporting Information).[22,23] The third-order rate constant k for $v = -k[Et_4NSH]^2$ was

(14) (a) McMaster, J.; Tunney, J. M.; Garner, C. D. *Prog. Inorg. Chem.* **2004**, *52*, 539. (b) Enemark, J. H.; Cooney, J. J. A.; Wang, J.-J.; Holm, R. H. *Chem. Rev.* **2004**, *104*, 1175. (c) Partyka, D. V.; Holm, R. H. *Inorg. Chem.* **2004**, *43*, 8609. (d) Sugimoto, H.; Tarumizu, M.; Tanaka, K.; Miyake, H.; Tsukube, H. *Dalton Trans.* **2005**, 3558. (e) Sugimoto, H.; Furukawa, Y.; Tarumizu, M.; Miyake, H.; Tanaka, K.; Tsukube, H. *Eur. J. Inorg. Chem.* **2005**, 3088. (f) Baba, K.; Okamura, T.; Yamamoto, H.; Yamamoto, T.; Ohama, M.; Ueyama, N. *Inorg. Chem.* **2006**, *45*, 8365.

(15) (a) Oku, H.; Ueyama, N.; Nakamura, A. *Inorg. Chem.* **1995**, *34*, 3667. (b) Lorber, C.; Donahue, J. P.; Goddard, C. A.; Nordlander, E.; Holm, R. H. *J. Am. Chem. Soc.* **1998**, *120*, 8102.

(16) Sugimoto, H.; Tajima, R.; Sakurai, T.; Ohi, H.; Miyake, H.; Itoh, S.; Tsukube, H. *Angew. Chem., Int. Ed.* **2006**, *45*, 3520.

(17) Because the m/z = 512 and 480 values correspond to these monoanionic states, one electron oxidation of the formed **1** and **3** may take place during the measurement. ESI-MS spectra of isolated $(Et_4N)_2[MoE_n(cyclohexene\text{-}1,2\text{-}dithiolate)_2]$ (n = 1, E = O, S; n = 2, E = O) in CH_3CN also gave peak clusters attributed to these monoanionic species.[19,20]

(18) ^1H NMR (CD_3CN, aromatic region): δ 6.38 (d, 1 H, for **1**), 6.46 (d, 1 H, for **1**), 6.56 (q, 4 H, for **3**), 6.71 (t, 2 H, for **1**), 6.94−7.09 (m, 5 H, for **1** and **3**), 7.10 (d, 1 H, for **1**), 7.20 (t, 2 H, for **1**).

(19) Sugimoto, H.; Harihara, M.; Shiro, M.; Sugimoto, K.; Tanaka, K.; Miyake, H.; Tsukube, H. *Inorg. Chem.* **2005**, *44*, 6386.

Scheme 1. Proposed Mechanism for the Conversion Process of **2**/**5** into 0.5 equiv of **1**/**4** and 0.5 equiv of **3**/**6** upon Reaction with 1 equiv of SH−

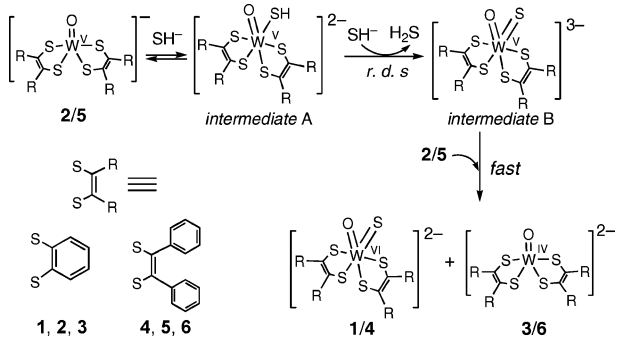

calculated to be 1.7×10^3 M^{-2} s^{-1} (Figures S2 and S3 in the Supporting Information). A possible mechanism for the conversion process is shown in Scheme 1. The reaction of **2**/**5** with SH^- generates SH^- adduct $[W^V(O)(SH)(dithiolene)_2]^{2-}$ (intermediate A), and another SH^- acts as a base to deprotonate from the SH group, producing $[W^V(O)(S)(dithiolene)_2]^{3-}$ (intermediate B). Then, redox reaction of the generated $[W^V(O)(S)(dithiolene)_2]^{3-}$ and another **2**/**5** quickly occurs to yield **1**/**4** and **3**/**5**. On the basis of the second-order dependence on the SH^- concentration, the deprotonation process may be the rate-determining step.[24]

The resonance Raman (rR) spectrum of a reaction solution of **2** and 1 equiv of Et_4NSH in CH_3CN showed one distinct band centered at 476 cm^{-1} (Figure 5). This was unambiguously assigned to the $\nu(W^{VI}{=}S)$ stretching band of **1** because the authentic sample of **3** did not exhibit any rR bands in this region when it was irradiated with a 632 nm He−Ne laser. The rR bands for $\nu(W^{VI}{=}O)$ and $\nu(W^{VI}{=}S)$ stretching bands of **4** appeared at 865 and 465 cm^{-1}, respectively (Figure S5 in the Supporting Information). The $\nu(W^{VI}{=}O)$ stretching band values of **1** and **4** are close to that of formaldehyde ferredoxin oxidoreductase (FOR; 874 cm^{-1}) in the AOR family,[25] suggesting that **1** and **4** serve as suitable active-site models. The lower $\nu(W^{VI}{=}O)$ and $\nu(W^{VI}{=}S)$ stretching band values of **1** and **4** than those of compounds listed in Table 1 except $[Cp^*W^{VI}(O)(S)(Se)]^-$ suggest that strong electron donation by the dianionic dithiolenes to the tungsten(VI) centers effectively decreases the terminal $O \rightarrow W^{VI}$ and $S \rightarrow W^{VI}$ donations, providing the weakened $W^{VI}{=}O$ and $W^{VI}{=}S$ bonds. Thus, complex **4** coordinated by stronger electron-donating dithiolenes $S_2C_2Ph_2$ than bdt gives weaker $W^{VI}{=}O$ and $W^{VI}{=}S$ bonds.

Complexes **1** and **4** were immediately converted to the corresponding $(Et_4N)_2[W^{VI}O_2(dithiolene)_2]$ in CH_3CN by adding a small amount of H_2O, as monitored by the UV−vis and ESI-MS (Figure S6 in the Supporting Information) spectral changes. The hydrolytic reaction well mimics an inactivation process found in active sites of the AOR family, where the active tungsten center is hydrolyzed to the inactive dioxotungsten(VI) center ($[W^{VI}O_2]^{2+}$) in the absence of sulfide.

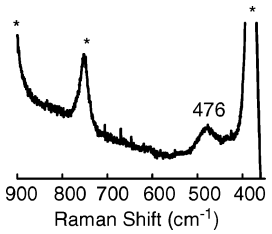

Figure 5. rR spectrum of a reaction solution of **2** (5.0×10^{-4} M) and 1 equiv of Et_4NSH in CH_3CN at room temperature using a He−Ne ion laser with excitation at 632 nm (asterisks indicate solvent peaks).

Table 1. Vibrational Frequencies (cm^{-1}) for Oxo−sulfidotungsten(VI) Complexes

complex	ν(W═O)	ν(W═S)
$(Et_4N)_2[W(O)(S)(bdt)_2]^a$ (**1**)	899 (IR)	476 (rR)
$(Et_4N)_2[W(O)(S)(S_2C_2Ph_2)_2]^a$ (**4**)	865 (rR)	465 (rR)
$(Et_4N)[W(O)(S)(OSiPr^i_3)(bdt)]^b$	949, 911 (IR)	477 (IR)
(*R*,*S*)-Tp*W(O)(S)(−)-mentholate^c	930 (IR)	480 (IR)
Tp*W(O)(S)(OPh)^c	935 (IR)	480 (IR)
Tp*W(O)(S)(SPh)^c	925 (IR)	480 (IR)
Cp*W(O)(S)$(CH_3)^d$	930 (IR)	497 (IR)
$W(O)(S)(OSiPh_3)_2(Me_4phen)^e$	933 (IR)	480 (IR)
$(Ph_4P)[Cp^*W(O)(S)(Se)]^f$	871 (IR)	450, 444 (IR)
FOR^g	874 (rR)	

[a] This work. [b] Reference 12. [c] Reference 9. [d] Reference 8. [e] Reference 10. [f] Reference 11. [g] Formaldehyde ferredoxin oxidoreductase.[5]

In summary, this paper reported the first in situ generation of oxo−sulfidobis(dithiolene)tungsten(VI) complexes that model the proposed active-site structure for the AOR family of tungsten enzymes. The complexes were characterized by UV−vis, ESI-MS, ^1H NMR, IR, and rR spectra and were found to mimic the coordination environment including the W═E (E = O, S) bond strengths and hydrolytic reactions of the tungsten center of the AOR family.

Acknowledgment. The authors are grateful to Professor Koji Tanaka and Dr. Tohru Wada of the Institute for Molecular Science for measurement of rR spectra. This work was supported by grants for Scientific Researches (Grants 18750052 and 19027048) from the Japan Society for Promotion of Science.

Supporting Information Available: Experimental details and first-order plots of the reactions of **2** with excess Et_4NSH (Figure S1), titration of **5** with Et_4NSH and time-dependent spectral changes for the reaction of **5** and excess Et_4NSH (Figure S2), first-order plots of the reactions of **5** with excess Et_4NSH (Figure S3), ESI-MS and rR spectra of a reaction solution of **5** and an equivalent of Et_4NSH (Figures S4 and S5), and the ESI-MS change of **1** to $(Et_4N)_2[W^{VI}O_2(bdt)_2]$ (Figure S6). This material is available free of charge via the Internet at http://pubs.acs.org.

IC7012733

(20) Sugimoto, H.; Sakurai, T.; Miyake, H.; Tanaka, K.; Tsukube, H. *Inorg. Chem*. **2005**, *44*, 6927.
(21) Goddard, C. A.; Holm, R. H. *Inorg. Chem*. **1999**, *38*, 5389.
(22) Because Et_4NSH is irreversibly oxidized at ca. −0.3 V vs SCE in CH_3CN, $[W^VO(dithiolene)_2]^-$ complexes, which exhibit a W^V/W^{IV} couple above −0.3 V, are stoichiometrically reduced to $[W^{IV}O(dithiolene)_2]^{2-}$ complexes upon reaction with 1 equiv of Et_4NSH. We observed that $(Et_4N)[W^VO(3,6\text{-dichloro-}1,2\text{-benzenedithiolate})_2]$ exhibiting a reversible W^V/W^{IV} redox process at −0.27 V vs SCE was reduced to the $(Et_4N)_2[W^{IV}O(3,6\text{-dichloro-}1,2\text{-benzenedithiolate})_2]$ with 1 equiv of Et_4NSH in CH_3CN.
(23) Because the ^1H NMR spectrum of a CD_3CN solution containing **5** and 1 equiv of SH^- showed much overlapped signals in the range from 6.5 to 7.5 ppm, these signals could not be assigned unambiguously.
(24) **2** is converted into 0.5 equiv of $(Et_4N)_2[W^{VI}O_2(bdt)_2]$ and 0.5 equiv of $(Et_4N)_2[W^{IV}O(bdt)_2]$ upon reaction with 1 equiv of Et_4NOH.
(25) Only rR spectrum of *Pyrococcus furiosus* FOR has been reported so far.[5]